Estimation of Mass and Lengths of Sintered Workpieces Using Machine Learning Models

David Massimo, Elias Ganthaler, Attaullah Buriro, Francesco Barile, Marco Moraschini, Anton Dignös, *Member, IEEE*, Thomas Villgrattner, *Member, IEEE*, Angelika Peer, *Member, IEEE*, and Francesco Ricci

***Abstract*— Powder metallurgy (PM) is the branch of metallurgy that deals with the design/production of near-net-shaped sintered workpieces with different shapes and characteristics. The produced sintered workpieces are used in the automotive, aviation, and aerospace industries, just to name a few. The quality of the produced sintered workpieces largely depends on powder compaction techniques and the accurate adjustments of process parameters. Currently, adjustments of these process parameters are done manually and thus resulting in laborious and time-intensive effort. To this end, this article explores the use of machine learning (ML) in the compaction process and proposes an accurate and lightweight ML-based pipeline to estimate the quality characteristics (QCs) of the produced workpieces in the PM domain. More specifically, it presents a pipeline for workpiece's mass and lengths estimation by exploiting some novel hand-crafted features and comparing well-selected ML prediction models, namely, random forest (RF), AdaBoost (ADA), and gradient boosting (GB). The chosen models are trained on a combination of features extracted from environmental and sensory raw data to estimate the mass and lengths of the next produced workpiece. We have implemented and evaluated our scheme on a dataset collected in a real production environment and we have found that GB is the most consistent and accurate one with the lowest root-mean-squared error (≈0.0886%). The results of extensive experimentation have proven the relevance of the selected features and the accuracy of GB.**

***Index Terms*— Compaction process, machine learning (ML), powder metallurgy (PM), quality characteristic (QC) estimation, sintering.**

I. Introduction

POWDER metallurgy (PM) deals with the production of workpieces from metal powder and involves various manufacturing processes for this purpose. The production of sintered workpieces accounts for the largest share by volume among all the PM manufacturing processes, e.g., metal 3-D printing, etc. This process deals with the necessary techniques and methods that help to produce solid metal-based products from metal powders. This whole production process typically involves specific powder production, its onward treatment and conditioning, consolidation steps involving pressure (compaction) and high temperatures (sintering), and some secondary treatments [1], [2]. The production of sintered workpieces is characterized by a near-net-shape production with varying shapes and little waste. Companies working in this domain often deal with narrow tolerance fields and acceptable cut-off values for these workpieces in the range of few 10 μm for the workpiece dimensions and few 100 μg for its mass. However, due to the variability of various factors, such as environmental (air pressure, ambient temperature, humidity, etc.) and operational (powder type, applied pressure during the compaction process, etc.), workpieces may be produced out of the predefined cut-off values. Needless to say, this out-of-tolerance production results in a waste of resources and consequently financial losses. Hence a dire need for quality characteristics (QCs) estimation and automatic process parameter adjustment is in order.

Machine learning (ML) is the branch of artificial intelligence that studies how computers can learn to solve a task without being explicitly programed [3]. ML models exploit real-world data as input, to develop autonomous decision-making abilities over time, such as learning to play a game or to recognize an object in an image. When these models are exposed to new (unseen) input data, they are required to generalize well: pretrained models (learned on previous computations on the input data) are expected to provide reliable and repeatable decisions on unseen data. Automating decision-making by using ML has already gained significant attention in recent years and use cases in banking (classification of the benign and fraudulent transaction [5]), healthcare (accurately monitoring the health of the patient [6]), and travel and transportation (hotel/visit recommender systems [21]) domains have been developed, just to name a few.

In sintered components production, a powder press machine is used to compact a loose mix of powder together into a so-called green part. The necessary compaction pressure for different-shaped workpieces is hereby applied by several independent punch levels following predefined trajectories. To guarantee the same quality of produced components/workpieces over a longer period, regular quality checks and manual trajectory adjustments are required—to cope with changing operating conditions due to environmental

Manuscript received 13 January 2023; revised 11 June 2023; accepted 5 July 2023. Date of publication 24 July 2023; date of current version 9 August 2023. This work was supported in part by the "RobuSinter" Project funded by the European Regional Development Fund (ERDF) under Project 1113. The Associate Editor coordinating the review process was Dr. Gaigai Cai. *(Corresponding author: Attaullah Buriro.)*

David Massimo, Elias Ganthaler, Attaullah Buriro, Francesco Barile, Marco Moraschini, Anton Dignös, Angelika Peer, and Francesco Ricci are with the Faculty of Engineering, Free University of Bozen-Bolzano, 39100 Bolzano, Italy (e-mail: aburiro@unibz.it).

Thomas Villgrattner is with GKN Sinter Metals, 39031 Bolzano, Italy.

Digital Object Identifier 10.1109/TIM.2023.3298413

and operational settings such as varying temperature, stroke rate, and powder quality [4], [7]. These adjustments are not only labor-intensive but also costly, hence often jeopardizing effective production.

Few research papers have demonstrated the suitability of ML models in the quality assessment of sintered components. These models have been employed for the estimation of mechanical and fatigue properties [22], [24], or density estimation of sintered bronze [23]. Here, we focus on the prediction of different QCs, i.e., mass and lengths, for more complex, i.e., multilevel, workpieces. More importantly, while in [22], [24], and [23] the input features used by the ML models are mainly limited to the composition of the alloy components and the static summary of the production process, here we design and utilize features that fully characterize the dynamics of the production process of sintered workpieces, regardless of the components' properties, to predict their QCs. Moreover, while previous works employ ML models based on artificial neural networks (ANNs), which require long training times and expensive optimization procedures to tune their hyper-parameters, here we show that QCs can be effectively predicted by harnessing simpler and more quickly trainable ML models, with lower computational time complexity. Hence, this article proposes a lightweight and accurate ML-based pipeline for estimating the aforementioned QCs of the workpieces. Our pipeline, first, extracts novel hand-crafted features from environmental and sensory data readings collected directly from sensors installed on the machine. More specifically, our approach leverages the fusion of environmental variables, e.g., room humidity, room temperature, pressure, etc., and the sensory readings captured directly from sensors installed on the press. Then, it exploits lightweight ML models since they are quick in training and estimating the QCs. Moreover, the used ML models are less resource and data-hungry, compared to other ML techniques, such as recurrent neural networks (RNNs). The chosen predictive models are trained and evaluated on the collected dataset. We have compared the performance of alternative models, and we have found that gradient boosting (GB) yields the lowest root-mean-squared error (RMSE) ($\approx$0.0886%) and consumes few microseconds ($\approx$300) to predict the required QCs. Our obtained results show the efficacy and the effectiveness of the proposed approach, based on ML prediction and feature selection. In fact, this article is the first one to analyze the impact of a vast number of features on the final estimation and to compare different ML algorithms in this special application domain. In summary, the main contributions of this article are as follows.

1) The proposal of an accurate and lightweight ML-based pipeline for mass and lengths estimation of the produced workpieces in the PM domain.
2) The proposal of a novel hand-crafted feature extraction process from low-level data signals, which are collected directly from the sensors installed on the press machine, and are generated during each stroke of the press. Furthermore, the identification of important features, with respect to their impact on the prediction of the QCs.
3) The experimental validation methodology used to assess the feasibility of the proposed lightweight method in producing accurate estimations of a workpiece's mass and lengths.

The rest of the article is structured as follows. Section II presents the general life cycle of a typical PM process and surveys the state-of-the-art in this domain. Section III summarizes our approach to the QCs estimation problem. Section IV presents the steps carried out to validate the approach. Section V summarizes the obtained results, followed by a discussion in Section VI. The article ends with Section VII presenting the summary of the article's contribution and possible future research directions.

II. Background and Related Work

A. PM Process

PM is a relatively small sector compared to other manufacturing industries, however, it has shown constant growth and increased importance in recent years. It involves multiple technologies to process metal powder and produce cost-efficient components of various types, shapes, and sizes. Alternate approaches, such as machining and casting, are costly and material/energy intensive for high-volume production.

The life cycle of a conventional PM process for structural press and sintered components consists of the following phases: powder production (mixing of powders with alloying elements), compaction (pressing powders to form a component), sintering (thermal treatment of the produced component), and final checks on the quality of the produced components. In Sections II-A1–II-A4, we explain the phases of the PM process for structural press and sintered components.

1) Metal Powder Production: Generally, all iron powders for parts production are manufactured by using iron-based powders with press additives. These iron-based particles are characterized by an irregular shape which is necessary for good compaction. To increase the compressibility, lubricants are added to the powder. By adding different metal powders and carbon, the final material properties can be adjusted. The different components of the powder mix are then mixed to make the powder ready for production [7], [8], [10].

2) Compaction: Compaction has the greatest technical importance in the production of sintered components. The so-called rigid die pressing is the most common way of pressing metal powder under high-pressure loads. The compaction press machine comprises a die, several upper and lower punch levels, and core rods. The process of compaction involves pressing the powder at room temperature (or elevated temperature below 200 °C) with the help of several punch levels. The required hardware is dependent on the geometry of the to-be-produced workpieces, e.g., to produce complex workpieces, several lower levels, core rods, upper levels, and a die are needed. Modern powder press machines have up to ten individual levels and are either hydraulically, mechanically, or electrically activated. Depending on the geometrical complexity, different press types are used.

At the beginning of each pressing cycle, the press cavity gets filled with metal powder, before it gets compacted under high-pressure loads to a so-called green part with almost half the initial powder's height. The green part gets removed in the last compaction phase and the press cycle begins again.

These highly precise compaction tools are normally made out of hardened and wear-resistant steel with a high-quality surface. The punches are inserted into each other.

3) Sintering: The output of the compaction process has sufficient strength to be moved to the next production step called sintering. Sintering is a thermal treatment with temperatures around 85% of the melting point of the main powder component under a controlled atmosphere. Surface diffusion is the driving force for individual particles to combine and form a solid body. The increased temperature leads to surface diffusion, which causes the individual particles to bond with each other increasing the workpiece strength. The sintering process takes place in three stages, during which the porosity and volume of the green compact are significantly reduced. In the first stage, only densification of the green compact takes place, whereas, in the second stage, the open porosity is significantly reduced. The final strength or hardness of the sintered components depends upon the sinter necks formed in the third stage, which are created by surface diffusion between the powder particles.

4) Quality Measurements: The produced workpieces need to satisfy the required QCs specifications after each production step. To pass the final quality check, they must be within the predefined specifications. The QCs including mass and lengths could be measured with a scale and micrometer, however, these continuous monitoring and iterative adjustments aimed to obtain the set of parameters to ensure the required quality are experience-dependent and manual. Hence, there is a dire need for an accurate method to estimate the QCs for further adjustments of process parameters.

B. Workpiece Mass and Lengths Estimation

In the determination of selected QCs, the literature focuses primarily on density determination. Analytical methods or FE-based methods can be used for this purpose. The former describes the so-called compaction curve using empirical equations as a function of the applied force. The average density of the component determined in this way can be calculated very quickly and with little effort. However, no similar equations have been presented in the literature to determine QCs such as dimensions or mass [25], [26]. The compaction process can also be simulated using the finite element method (FEM), which uses a material law to calculate the stress–strain relation. Most of these papers use the material density during the compaction as an internal variable. In contrast to the analytical equations, local stresses or densities can be determined, coming with the cost of high computational effort and cost. Finite element-based simulation software has been shown to be highly accurate [14], [16], [27], however, being off-line and computationally expensive, they are not considered for on-line (in real-time industrial settings) estimations.

This article proposes a lightweight and accurate ML-based pipeline for estimating the QCs of the produced workpieces. First, it proposes a novel hand-crafted feature extraction process for machine signals, collected directly from the press machine. Then, it exploits lightweight and quick ML models to estimate with high precision the QCs of the produced workpieces. Furthermore, this work is the first one comparing different ML models and looking more systematically at the feature construction and selection, which are steps that play an important role in quality estimation.

TABLE I
CONTROL AND TOLERANCE LIMITS FOR THE QCs

Quality characteristic	Lower tolerance	Set value	Upper tolerance
Mass (g)	16.1	16.3	16.5
Length 1 (mm)	2.2	2.25	2.3
Length 2 (mm)	4.44	4.49	4.54
Length 3 (mm)	6.68	6.73	6.78
Length 4 (mm)	8.92	8.97	9.02

III. ML-Based QCs Estimation

A. Specification of Test Workpiece

We aim to identify the process parameters having a dominant influence on the QCs of the produced workpieces (see Fig. 1) and to generate a reliable prediction of the desired QCs, that is, the workpiece's mass and lengths. We are interested in estimating the QCs of the complex workpiece shown in Fig. 1. As we have mentioned before, this is a preliminary step to be able to automate the process parameter adjustments as part of future work.

Table I shows the tolerance limits for the mass and the lengths of the target workpiece. We need to ensure that the estimated mass and the other four QCs, namely, Lengths 1–4 [see Fig. 1(b)], also remain within the limits specified in Table I. In fact, the produced workpiece is considered of good quality if its estimated mass and lengths stay within the specified limits, possibly as close as possible to the set value (the ideal value of the QCs of the part).

B. Quality Estimation Approach

The production of sintered components depends upon several production, material, and environmental parameters. For example, changes in the press stroke rate lead to changes in the tool temperature and dynamics of the different punch levels and feeding shoes. For this reason, we performed experiments with changing stroke rates (27, 31, and 35 strokes/min) on different experimental days. Furthermore, during the entire data collection phase, we ensured that the process starts and remains within the tolerance limits. This experimental design was chosen in agreement with process experts from the production site in our partner company in order to be able to map the effect of different machine dynamics with the associated tool temperature changes as well as the influence of environmental parameters, while not changing any machine settings.

We would like to highlight that temperature changes in our experiment are also due to the manipulation of the order in which the stroke rate varies during production (e.g., going from a stroke rate of 35–31 and then 27). At stroke rate 35, we observed the highest tool temperature, whereas at stroke rate 27 the lowest. That said, in the experiment tool

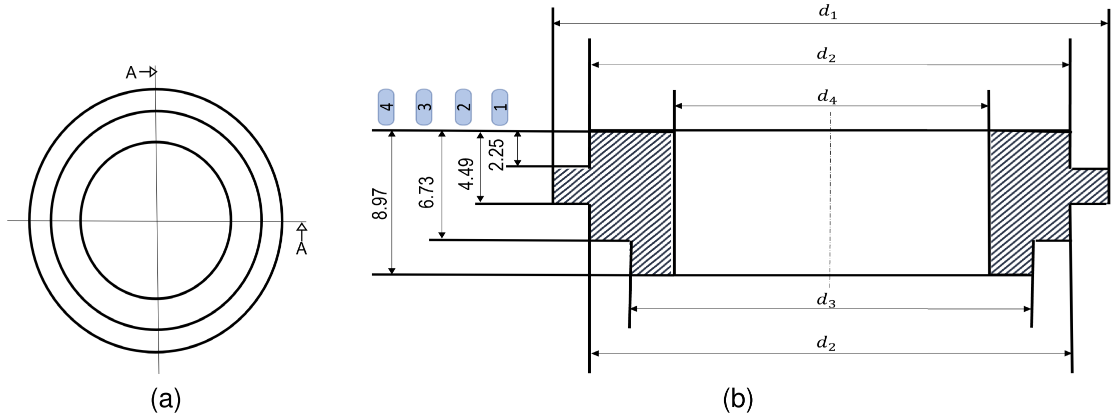

Fig. 1. (a) Desired workpiece in top view and (b) its dimensions in AA section. The four different QCs for the length (in mm) are highlighted in blue.

temperature changes in relation to the machine dynamics. The decision for different production days was taken to cover a wider range of environmental changes, hence resulting in a richer dataset.

The collected data is divided into press-curve-dependent and environmental data sets. We note that they have different timestamps. Press-curve-dependent data are acquired by sensors that measure properties (e.g., position) of the press tools, while environmental data are sampled by sensors measuring environment characteristics (e.g., temperature). Therefore, we dedicate the first step of our approach to data alignment. In the next step, we automatically extract statistical features from the aligned raw data. The full dataset is partitioned into three sets, i.e., training, validation, and testing. We exploited training and validation datasets for empirical comparison of the chosen ML models and to choose the most accurate to test on the unseen data. Fig. 2 illustrates our approach as a block diagram.

IV. Experimental Evaluation

A. Data Sources

Our dataset includes temporally dependent recorded values from various sources, i.e., press levels on the machine, the environmental sensor recordings, the physical characteristics of the produced workpiece, and the powder type used during the compaction process. In this analysis, we use press-curve data (representing signals recorded at regular intervals from the compaction press during the manufacturing process) and environment data, i.e., temperature and humidity (acquired with a fixed sample rate independent of the production cycle). The used compaction press machine is equipped with built-in low-level closed-loop controllers using a sample rate of 2 kHz. For this purpose, the manufacturer added dedicated sensors, e.g., for position and force, for every single level. These sensors provide the required resolution in terms of amplitude and sampling rate so that workpieces can be produced with high relative accuracy. However, due to compaction tool mounting offsets, different powder behavior, and changing environmental conditions, the absolute accuracy of the produced parts may change over time and needs to be estimated with the introduced ML models.

Furthermore, the company added sensors for measuring air pressure, relative humidity, absolute humidity, and ambient temperature to acquire environmental data. Since the environmental conditions change with a much lower frequency (compared, for instance, to the position of the punch levels during production), a sampling rate of 1 Hz is used.

We extract a fixed number of recordings for each punch level during the production of each produced workpiece (more on this is detailed later) along with the type of material (powder type) and the frequency of press in terms of number of produced workpieces per minute (stroke rate). These recordings define the press cycle completion process of a workpiece. We take the recordings at different percentages of the full cycle of production of a single workpiece; capturing data at various stages from the initiation to the completion of the press cycle, hence we operate in the press cycle range between 0% and 100%.

Finally, we have the ground truth in terms of "quality data" (masses and lengths of produced workpieces). These ground truth measurements are made by a sophisticated measurement device—a laser triangulation system is used to scan the produced pieces to extract geometrical information (lengths), and a scale to extract the mass of the produced workpieces. The laser triangulation system has a linearity of $\pm 0.006\%$ and a repeatability of 0.4 μm, while the scale has a resolution of 1 mg and repeatability of 2 mg.

QCs data is also acquired for every workpiece and it is used to train the considered ML models for the prediction of QCs and to verify the predicted QCs. Please, note that verification (test) data are not used during the model training and the parameter optimization processes.

It is worth noting that our dataset also contains information about the quantity of powder used in the experiment which remained constant throughout this experimental setting, and hence is not used for analysis. In addition, our processing data pipeline assesses the variability of the recorded values based on the variations in the machine's stroke rate. Moreover, the number of produced pieces, whose data are collected, is not high: there are around 200 pieces per experimental condition, hence there is not much variability in the filling level value of the container during the experiments. The filling level information might be useful with long-term experiments

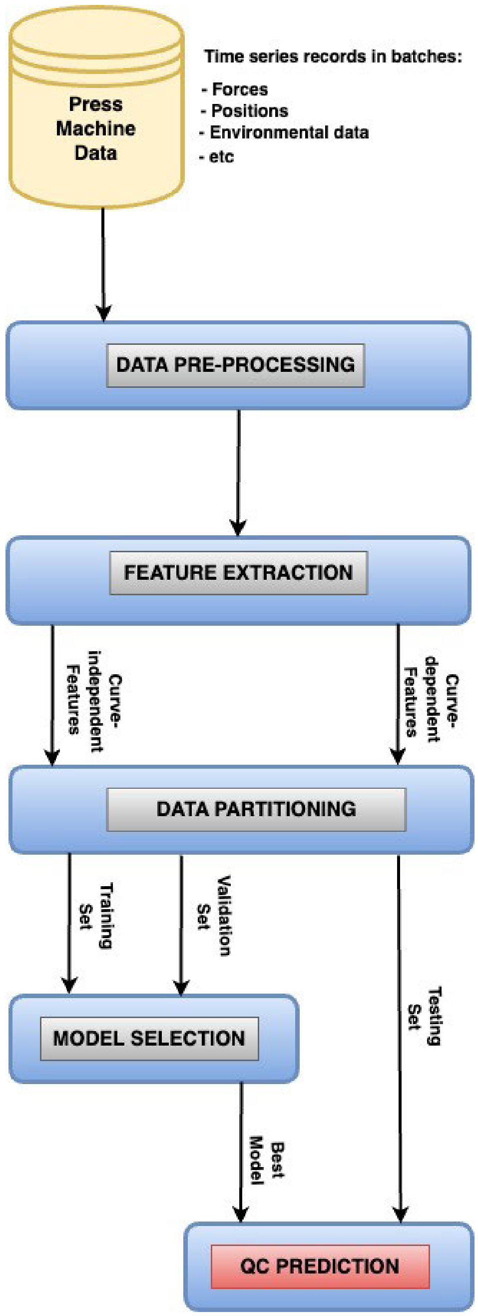

Fig. 2. Block diagram of our approach.

where tens of thousands of workpieces are produced. In this case, changes in the filling level could become more evident.

B. Data Processing

Data processing is the process of synchronizing the collected data from different sources and converting them into an organized form. It is specifically needed when the data is collected from multiple sources. This processed data needs to be arranged in a way that could be beneficial to serve the purpose of data analysis. In fact, the chosen model is expected to work better on the processed data as compared to the raw data, hence, resulting in better decisions, higher accuracy, and increased reliability. Overall, this step eases data storage, analysis, and presentation.

In this section, we explain the steps implemented to process the raw data, collected from different data sources.

1) Considered Variables: We recall that due to the complex shape of the desired workpiece, there is a diverse combination of tools: top-ram (TR), upper level 2 (UL2), lower levels (LL1–LL3), die, and filler. Tools attached to the press, are installed at different hydraulic cylinders, which we refer them as levels, and are following predefined trajectories to produce a workpiece, as, for instance, that depicted in Fig. 1(b).

By plotting the position of a level for a fixed stroke rate over a press cycle (in the range 0%–100%), we obtain its trajectory, which encompasses the different phases of the press cycle (blue line in Fig. 3). A trajectory describes a stroke, which produces a workpiece. Fillers in the PM domain, are used to fill the powder products into different cavities of different forms. These powders are then compressed with extra pressure from different dimensions to create the desired shape.

For our analysis, we considered the following variables, which by means of the above-mentioned sensors, record specific properties of the tools attached to the press levels.

1) Actual and desired positions of TR, LL1, LL2, LL3, UL2, and Filler.
2) Actual forces of TR, LL1, LL2, LL3, and UL2.
3) Hydraulic pressure.

Hydraulic oil is used to drive the hydraulic cylinders and the punches mounted on them. When several punches need to be moved at the same time, pressure drops, and recovery can be observed which changes with the experimental settings. Thus, we record also the hydraulic pressure. Besides the recorded data listed above, the absolute humidity and work of each punch level are calculated. We compute the work of a punch level using the standard formula, as follows:

$$W = F\,\Delta x \tag{1}$$

where W is work, F is the force in newton (N), and Δx change in position (meters). Work W is measured in joules (J).

We performed a first preliminary analysis of the environment and press-curve variables to check if the recorded data was reliable. Environment data was collected from dedicated sensors, i.e., thermometers, and barometers, installed on, or close, to the press machine. To obtain reliable readings, temperature sensors are glued on the tools close to the compaction zone. As a result of this analysis, we have removed unsuitable variables that were found to be either constant or noninformative. For instance, we found constant environmental data, e.g., the temperature of TR, when the wire of the temperature sensor was found to be broken.

In short, we exploit the following environmental variables for our analysis.

1) Air pressure environment.
2) Relative humidity environment.
3) Temperature environment.
4) Temperature UL, LL, and die.

Moreover, for some strokes, we identified missing values in the collected press-curve dataset. In this case, we computed

TABLE II

VARIABLES USED IN THIS ANALYSIS

Quality data	Mass, Lengths
Press-curve	Hydraulic pressure, Filler position actual, Filler position desired, TR position actual, TR force actual, TR position desired, LL1 position actual, LL1 force actual, LL1 position desired, LL2 position actual, LL2 force actual, LL2 position desired, LL3 position actual, LL3 force actual, LL3 position desired, UL2 position actual, UL2 force actual, UL2 position desired, LL1 work, LL2 work, LL3 work, TR work, UL2 work
Environmental data	Air Pressure Env, Relative Humidity Env, Absolute Humidity Env, Temperature Env
Tool temperatures	Temperature UL, Temperature LL, Temperature DIE
Experiment setting	Powder, Stroke rate

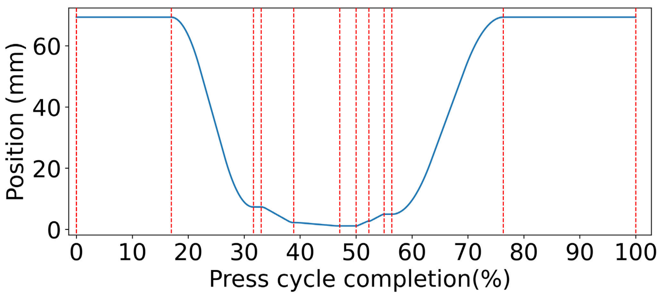

Fig. 3. Partition limits (red lines) on the variable "TR position actual." In blue is described the value of this variable during the production cycle of one workpiece.

the mean of all the previously collected data samples and added them in the missing value columns. This is a common approach in ML and has been widely used when dealing with missing values in sensor-augmented settings (e.g., smart cities and smart factories) [18].

In Table II, we list the press-curve and environmental variables (environmental data and tool temperatures) considered in the study, the variables characterizing the experimental setting (experimental setting), and the target variables (quality data).

2) Feature Extraction: Here, we discuss the methodology we have applied to extract features from press-curve variables. For each recorded stroke we divide each sequence of temporally dependent press-curve variable data into different partitions, and then for each partition, we compute features, by aggregating data readings in each partition. Partitions are identified by their limits: the start and the end of the partition. Each partition contains sensor data corresponding to different operations, i.e., filling, compaction, ejection, and removal performed by the tools during the press cycle. In Fig. 3, we show with vertical red lines the partition limits for the variable "TR position actual." In Fig. 4, we show the partitions defined for the position variable of each press level and the corresponding press cycle phase. It is important to note that environmental variables are not processed into features because they do not depend on partitions.

Starting from the considered press-curve variables, we could generate the following features. By considering the six tools/levels (TR, UL2, LL1, LL2, LL3, and F), in total 68 partitions are created (see Fig. 4). Then, for each partition, four press-curve readings (actual and desired position, actual force, and hydraulic pressure) are considered. Finally, for all these 68 $\times$ 4 combinations, we create features by using five

TABLE III

NUMBER OF CONSIDERED STROKES/WORKPIECES AND FEATURES AFTER THE CLEANING AND PROCESSING OPERATIONS

# Strokes	5667
# Press curve features	1039
# Cycle independent features	7
# of data points	5.9×10^6

aggregation operations on the time-dependent values of the variable in a partition: mean, standard deviation, maximum, minimum, and power spectrum deformation. Hence, by considering the press-curve variables, the total number of features that could be generated for representing a workpiece is 1360. Some of the features (precisely 321), computed on ill-formed raw data (e.g., duplicate, incorrect, and/or constant), were removed, hence the final feature vector created from press-curve data is 1039-features long. Furthermore, we add the seven considered environmental features to construct the final feature vector of 1046 features.

We also note that in our experiment, by varying the powder type and the stroke rate, we have produced 5667 workpieces (one for each stroke) and for each of them we have applied the aforementioned feature extraction procedure. The number of produced workpieces and features after cleaning, processing, and feature extraction of the datasets are shown in Table III.

Since, for each of the produced workpieces, we have a 1-D real-valued vector of size 1046, whose values correspond to the specific features, the resulting dataset consists of over 5.9 million data points. Without applying the cleaning stage in the feature extraction process, the dataset would have been 24% larger, i.e., containing 7.7 million data points. Each vector representation of a workpiece is then used to predict mass and lengths. We would like to highlight that for the prediction we use five distinct instances of the same ML model type: one to predict the mass and the other four to predict the four characteristic lengths of the workpiece (see Fig. 1). To conduct the prediction task, we further reduce the dataset size by selecting the most appropriate features for each model (see Section IV-D). In Fig. 5, we illustrate the input of the prediction (feature vector), the output of the prediction task, and its evaluation.

C. Serial Correlation Effect Analysis

We have analyzed the masses of the produced pieces to investigate whether a serial correlation exists, i.e., if the mass of a workpiece is correlated with the masses of the

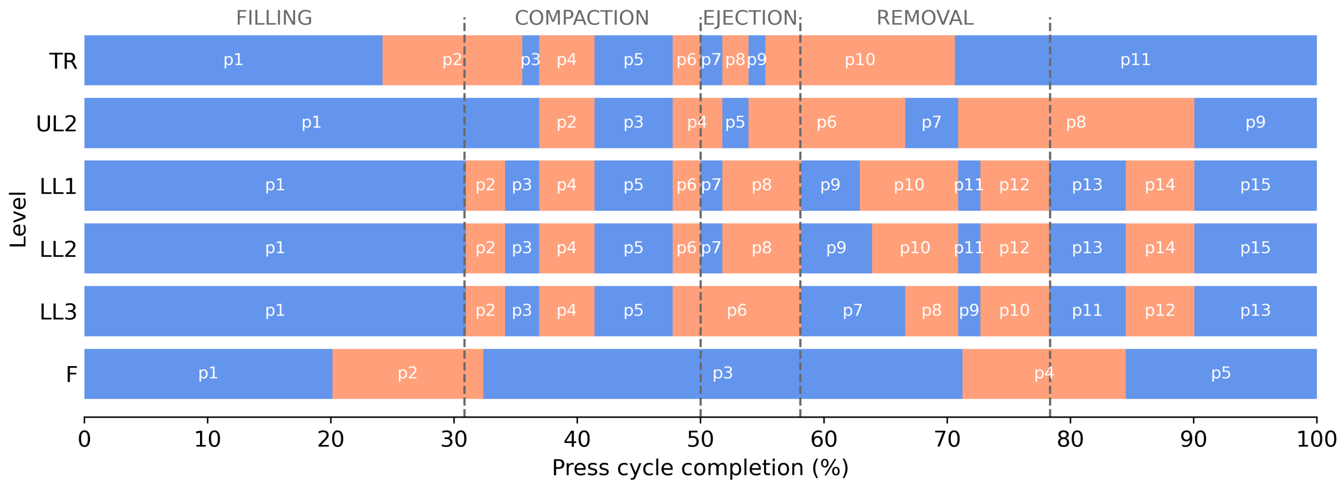

Fig. 4. Partitions of the position variable for each level and press cycle phases.

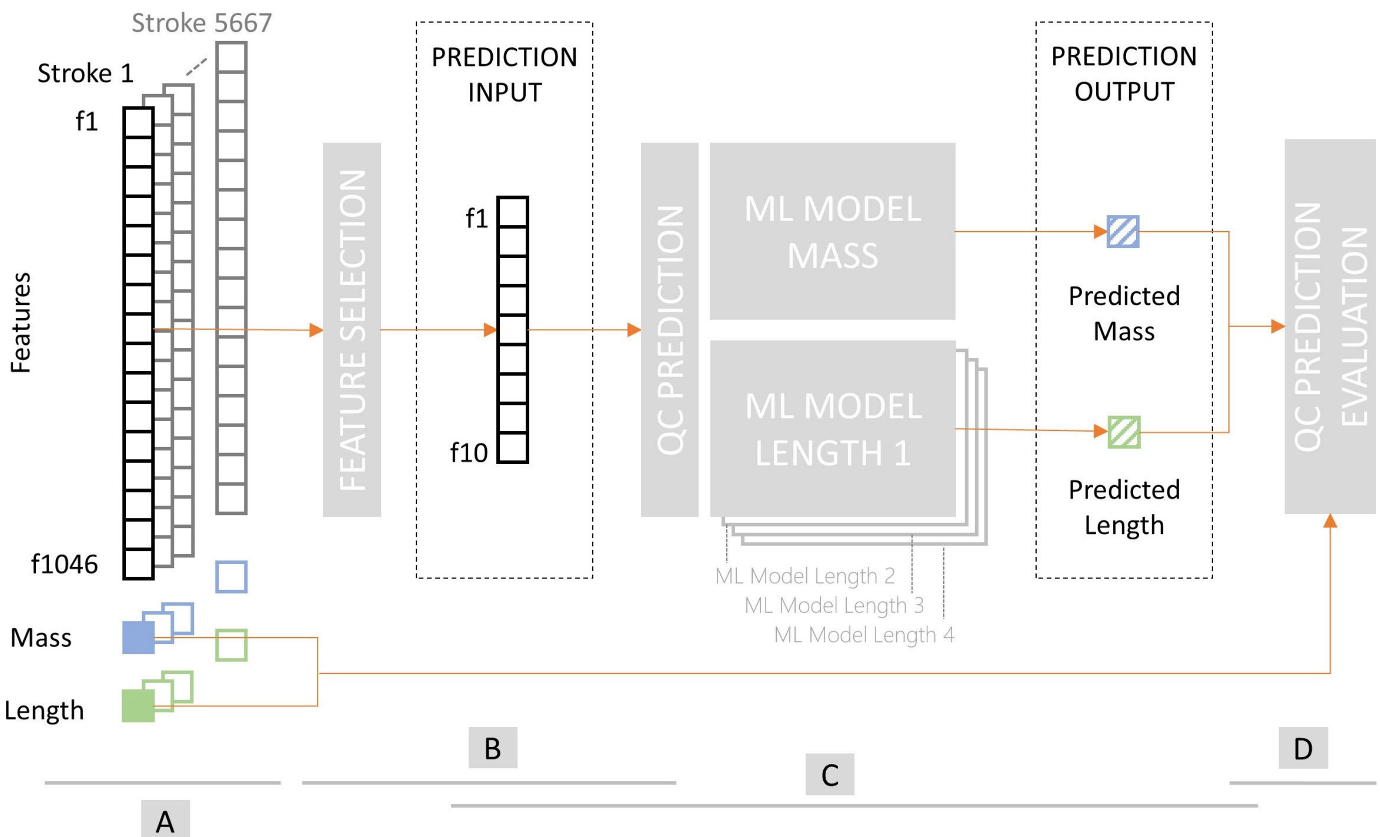

Fig. 5. (A) Feature vectors and target quality data to predict. (B) Feature selection process and resulting feature vector for quality data prediction. (C) Input of the prediction, ML models, and prediction output. (D) Prediction evaluation and inputs.

previously produced pieces. We have used the Ljung–Box test to perform this check since it is a widely used method for testing serial correlations. The test hypotheses are defined as follows: *H0*: the data point are independently distributed (i.e., the correlations in the population from which the sample is taken are 0, so that any observed correlations in the data result from the randomness of the sampling process). *Ha*: the data points are not independently distributed; they show serial correlation.

We then checked the serial correlation by using the production batches. We found that over 90% of the batches show a test statistic (p-value) lower than 0.05. Hence we conclude that serial correlation exists and must be considered in evaluating the predictive models. Therefore, we can not randomly partition strokes into training and testing sets, as with this approach one would overestimate the performance of the model. Conversely, we used the time-based data split strategy presented in Section IV-E.

TABLE IV
INTERPRETATION OF THE CORRELATION VALUES

Correlation value	Correlation interpretation
0.9 to 1.0 (-0.9 to -1.0)	Very high positive (negative)
0.7 to 0.9 (-0.7 to -0.9)	High positive (negative)
0.5 to 0.7 (-0.5 to -0.7)	Positive (negative)
0.3 to 0.5 (-0.3 to -0.5)	Moderate positive (negative)
0.0 to 0.3 (-0.0 to -0.3)	Low positive (negative)

D. Features Selection and QCs Correlation

To select a reduced amount of relevant features (from the original 1046) to represent each workpiece, and be used as input of the ML models to predict QCs, we perform a correlation analysis between the features and the QCs. In this way, we identify the set of features having the largest impact on the quality of the produced workpieces. We use the Pearson correlation coefficient [20] which is the most common way of measuring the correlation between variables. As shown in Fig. 5 (step B), from the initial feature vector of size 1046 features we select the top-ten most correlated. Hence, we generate five feature vectors of size 10. The first vector consists of the top-ten features correlated with the target mass and is used as input of the ML model to predict the mass [see Fig. 5 (step C)]. The remaining four vectors have as elements the top-ten features correlated with the four lengths, respectively. Each vector is used as input for the corresponding ML model, e.g., the feature vector containing the most correlated features with Length 1 is used with the ML model to predict Length 1.

In Table IV, we describe the interpretation of the correlation values that we utilize. While in Table V, we show the top-three features, in the two groups of press curve and environment features, according to their correlation to the considered QCs.

In summary, the top press-curve features correlated with the mass QCs are related to the removal of the workpiece from the press, i.e., features computed for the lower levels LL2 and LL3 in the partitions p10 and p12 (see Fig. 4), and the position of the UL2 at partition p9, which was found to be the feature most correlated with the final mass of the workpiece. Please note that removing a workpiece from the press is executed in parallel to the filling phase of the subsequent component to be produced. This implies that features related to the removal of the current workpiece are correlated with the filling of the next workpiece.

By looking instead at the correlations between press curve features and the workpiece's lengths we note that features related to force during the ejection and workpiece removal phases are the most correlated ones. Higher ejection forces are an indicator for increased axial and radial relaxation, also known as the spring-back factor, due to high compaction pressure.

If we now look at the correlation between the environment features and the QCs (see Table V), we see that environmental variables have a low positive correlation with Length 1 and a low negative correlation with mass, Length 2, and Length 4. A moderate negative correlation exists between environmental variables and Length 3. We explain the negative correlation by referring to the powder composition. A powder is a mix of iron

TABLE V
TOP-THREE FEATURES, IN THE GROUPS OF PRESS CURVE AND ENVIRONMENT, CORRELATED TO THE QCS. IN PARENTHESIS, WE INDICATE THE DEGREE OF CORRELATION, BASED ON THE INTERPRETATION OF ACTUAL VALUES FROM TABLE IV

Feature	Mass
Press curve	UL2_pos_z_actual - mean - p9 (High Positive) LL3_force_actual - std - p12 (Positive) LL2_position_z_actual - amax - p10 (Positive)
Environment	temperature_UL (Low Negative) temperature_LL (Low Negative) temperature_DIE (Low Negative)
	Length 1
Press curve	LL1_force_actual - amax - p7 (High Positive) TR_force_actual - amax - p6 (Positive) LL3_force_actual - amin - p6 (Positive)
Environment	relative_humidity_env. (Low Positive) temperature_LL (Low Positive) temperature_DIE (Low Positive)
	Length 2
Press curve	TR_force_actual - amin - p8 (Positive) TR_force_actual - mean - p8 (Positive) LL3_force_actual - amin - p6 (Positive)
Environment	relative_humidity_env. (Low Negative) temperature_LL (Low Negative) absolute_humidity_env. (Low Negative)
	Length 3
Press curve	TR_force_actual - amin - p8 (High Positive) TR_force_actual - mean - p8 (Positive) LL1_pos_z_actual - mean - p11 (Positive)
Environment	relative_humidity_env. (Moderate Negative) temperature_env.(Moderate Negative) air_pressure_env. (Moderate Negative)
	Length 4
Press curve	TR_force_actual - amin - p8 (High Positive) LL3_force_actual - amin - p6 (Positive) TR_force_actual - mean - p8 (Positive)
Environment	relative_humidity_env. (Low Negative) temperature_LL (Low Negative) temperature_DIE (Low Negative)

and press-additives such as lubricant particles; hence the only component of the powder that is highly variable according to the environmental conditions is the lubricant. When the humidity increases, the lubricant particles attract humidity and increase the cohesion work density leading finally to changing compressibility.

E. ML-Based Analysis Methodology

We now summarize the methodology that we have followed to identify the best-performing ML model for each QC. We have first divided the data into 15 batches. Each batch corresponds to a separate experiment based on powder and stroke rate settings. Since there are three powder types and five ordered stroke rates (35, 31, 27, 31, and 35 strokes/min), we ended up creating a total of 15 batches. Each batch, on average, contains data for 200 strokes/workpieces. Then, we divide each batch into three subsets: training, validation, and test. By using that data split, we then have run an optimization procedure using various models and various hyperparameters. Hyperparameter optimization refers to the selection of optimal hyperparameters for a learning algorithm. A hyperparameter is simply a parameter whose value is used to control the learning process. Hyperparameters are extremely important because they directly control the behavior of the training algorithm and have a significant impact on the performance of the model being trained. Hence, choosing

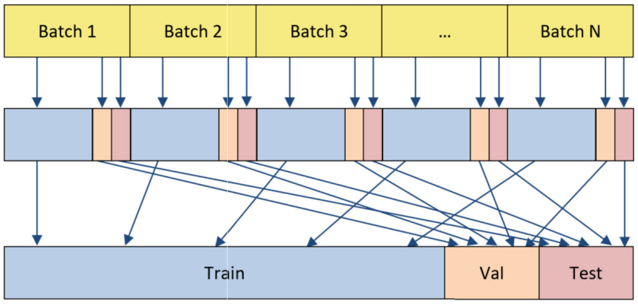

Fig. 6. Strategy used to split the dataset in the training, validation, and test sets.

appropriate hyperparameters plays a crucial role in the generalization capability of the trained model.

Fig. 6 shows the diagram of the data splitting procedure: we split each batch by taking the first 70% of the examples for training, the next 15% for validation, and the remaining 15% for testing. Afterward, we combine all the training, validation, and testing samples (extracted from each individual batch) to create the final training, validation, and testing sets for onward model training. We consider this approach of combining samples from individual batches more realistic than dividing the 15 batches in three splits, e.g., initial ten for training, two for validation, and the last three for testing, because this approach guarantees: 1) more model generalization capability and 2) better replicates the real-world production scenario.

We chose to use random forest (RF) [28], AdaBoost (ADA) [29], and GB trees [30] for several reasons. First, these algorithms are widely recognized and extensively used in ML for classification and regression tasks. They have been shown to have robust performance and to be effective in various domains. Second, these algorithms possess unique characteristics that make them suitable for specific problems, for example, RF is known for its ability to handle both low and high-dimensional datasets, handle irrelevant features, and provide good generalization. ADA, on the other hand, excels in boosting weak learners and reducing bias. GB is particularly useful in capturing complex interactions and producing accurate predictions. All in all, these models are extremely robust to overfitting, are generally accurate, and are reported to be among the top-ten algorithms [31] ML specialists should know.

We have analyzed the performance of our chosen ML models by varying the hyperparameters' values as follows.

1) RF.
   a) *Number of Trees:* From 50 to 800 at steps of 50.
   b) *Max Depth:* From 10 to 100 at steps of 10 plus "unlimited."
2) ADA.
   a) *Base Estimator:* Decision Tree three levels deep, decision Tree only one level deep.
   b) *Number of Trees:* From two to 400 at steps of 25.
   c) *Learning Rate:* 20 equally spaced values on a log scale from 10^{-4} to 100.5.
3) GB trees.
   a) *Number of Trees:* From 50 to 800 at steps of 50.
   b) *Learning Rate:* 20 equally spaced values on a log scale from 10^{-4} to 100.5.
   c) *Maximum Depth of Each Tree:* From 1 to 20 at steps of 3.

We have trained these models by using the top-ten features that showed a high correlation with the target QC. Hence, there are five feature vectors, one for each QC, that are used as input to a specific ML model (as detailed in Section IV-D).

We use the RMSE as the validation metric, to decide which hyperparameters (for each model) have the best performance on the 15% validation set (see Fig. 6). In Section V, we show the models' performance on the unseen test set, which is obtained by retraining the models on the union of the training and validation set. The used implementation of the ML models used in this article comes from the Python library scikit-learn [19].

V. Results

We report the results of the compared ML models by using standard metrics: RMSE, R^2, RMSE (%), and Pearson correlation (Corr).

RMSE is a commonly used metric to measure the average magnitude of the differences between predicted and actual values in a regression task. RMSE provides a measure of the overall accuracy of a regression model

$$\mathrm{RMSE} = \sqrt{\frac{\Sigma_{i=1}^{n}(x_i - \bar{x}_i)}{n}} \tag{2}$$

where $x_1, x_2, \ldots, x_n$ is the array of values for the quality parameter we are predicting, while $\bar{x}_1, \bar{x}_2, \ldots, \bar{x}_n$ are the corresponding predictions.

R^2 or R-squared measures the proportion of the variance in the dependent variable (mass or lengths) that can be explained by the independent variables (features) in the regression model. It provides an indication of the goodness-of-fit (in the range of 0–1 with a higher value indicating a better fit.) of the model to the observed data.

RMSE (%) offers a standard approach to quantify the error of a model so that comparisons of different prediction tasks can be performed. It is defined as follows:

$$\mathrm{RMSE}(\%) = 100 \cdot \sqrt{\frac{\Sigma_{i=1}^{n}\left(\frac{x_i - \bar{x}_i}{x_i}\right)}{n}} \tag{3}$$

where $x_1, x_2, \ldots, x_n$ is the array of values for the quality parameter we are predicting, while $\bar{x}_1, \bar{x}_2, \ldots, \bar{x}_n$ are the corresponding predictions.

Pearson correlation (Corr) measures the linear relationship between the predicted and true value of a QC (mass or lengths).

In addition, we report the training time (the average time taken to train the model across multiple experiments) and the prediction time (the computational time needed to predict a single QC).

We have performed our experiments on a server computer equipped with an Intel[1] Xeon[1] X5550 CPU (for a total of

[1]Trademarked.

TABLE VI

PERFORMANCE ON THE TEST SET OF THE ML MODELS IN PREDICTING THE WORKPIECE MASS, BY USING PRESS CURVE AND ENVIRONMENTAL DATA. THE BEST MODEL IS IN BOLD FACE

Model	RMSE	RMSE(%)	R^2	Corr
RF	0.0255	0.1570	0.9154	0.9575
Ada	0.0261	0.1609	0.9112	0.9587
GB	**0.0237**	**0.1460**	**0.9268**	**0.9630**

TABLE VII

FEATURE IMPORTANCE IN GB MODEL (BEST MODEL)

Rank	Feature
1	LL2_force_actual - mean - p9
2	LL1_force_actual - amax - p7
3	temperature_UL
4	air_pressure_environment
5	LL1_work - std - p5
6	LL2_work - std - p11
7	temperature_environment
8	relative_humidity_environment
9	LL1_work - mean - p5
10	LL2_work - mean - p9

TABLE VIII

TRAINING AND PREDICTION TIMES IN SECONDS FOR THE THREE MODELS CONFIGURED WITH THE BEST PARAMETERS FOR MASS QC ON COMBINED PRESS CURVE AND ENVIRONMENT FEATURES

Model	Training	Prediction (avg)	Prediction (std)
RF	17.4089	0.0218	0.0009
Ada	1.9068	0.0223	0.0003
GB	26.1311	0.0004	0

16 cores) and 40 GB of random access memory (RAM). Training and prediction tasks are performed by using a single core of the server CPU and by limiting the RAM usage to 8 GB. In this way, we can better compare the obtained model performance with that obtainable on an industrial PC (IPC).

A. ML-Based Prediction of Mass

As a result of the cross-validation parameter selection procedure, we have found that GB is the best-performing model (as depicted in Table VI); with hyperparameters configuration: learning rate of 0.02335, maximum depth of 4, and 750 estimators.

In Table VI, we show the performance of all the considered models in terms of our chosen metrics, when they are using their best hyperparameters' values, and are evaluated on the unseen test set. Moreover, in Table VII, we show the ranking of the ten predictive features describing a workpiece, based on their importance in predicting the mass QC in the best-performing ML model, that is, GB. While in Fig. 7, we show the comparison of true and predicted mass values, for each workpiece in the test set, for the best-performing model, i.e., GB.

Finally, Table VIII shows the training and prediction times of the considered models. All the models took less than a tenth of a second to predict the mass, and among them, GB is the quickest (≈300–400 μs).

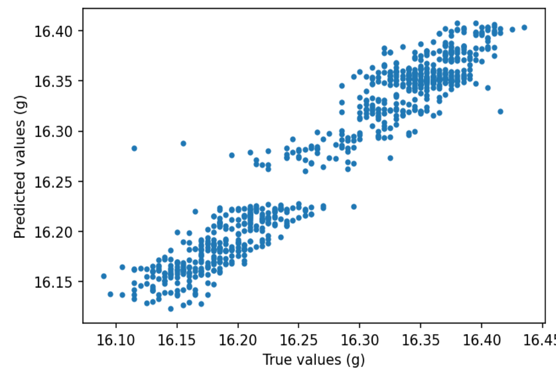

Fig. 7. Comparison between the predicted and true mass values of each workpiece in the test set: gradient boosted model and combined environment and press curve features.

TABLE IX

PERFORMANCE ON THE TEST SET OF THE PREDICTION OF THE LENGTH QCS, BY USING THE PRESS CURVE AND THE ENVIRONMENTAL FEATURES. THE BEST MODEL IS MARKED IN BOLD LETTERS

Model	RMSE	RMSE(%)	R^2	Corr
Length 1				
RF	**0.0031**	0.1390	0.7824	0.9020
Ada	0.0034	0.1525	0.7378	0.8827
GB	0.0032	0.1445	0.7645	0.8862
Length 2				
Model	**RMSE**	**RMSE (%)**	**R^2**	**Corr**
RF	**0.0095**	0.2119	0.6439	0.8054
Ada	0.0096	0.2132	0.6386	0.8120
GB	0.0096	0.2135	0.6388	0.8090
Length 3				
Model	**RMSE**	**RMSE (%)**	**R^2**	**Corr**
RF	0.0081	0.1209	0.7655	0.8794
Ada	**0.0080**	0.1195	0.7706	0.8822
GB	**0.0080**	0.1186	0.7743	0.8843
Length 4				
Model	**RMSE**	**RMSE (%)**	**R^2**	**Corr**
RF	**0.0079**	0.0879	0.8728	0.9384
Ada	0.0093	0.1030	0.8255	0.9348
GB	**0.0079**	0.0885	0.8712	0.9359

B. ML-Based Prediction of the Lengths

In Table IX, we show the performance of the considered ML models for length estimations, when their best hyperparameters' values are used, and they are evaluated on the test set. The best configuration of the considered models to predict the lengths QCs, determined via cross-validation and evaluation of the model performance on the validation set, are as follows.

- Length 1 RF with maximum depth 10 and 100 estimators.
- Length 2 RF with maximum depth 10 and 150 estimators.
- Length 3 GB with a maximum depth of 4 and 400 estimators and a learning rate of 0.0403.
- Length 4 GB with a maximum depth of 7 and 700 estimators, and a learning rate of 0.0136.

If we look at the model's errors, in terms of RMSE (%), as shown in Table IX, we can note that the models perform similarly when predicting the three lengths, namely, Lengths 1, 3, and 4, and worse for Length 2.

Finally, Table X shows the execution time of the models to predict the lengths QCs. The worst case requires less than a tenth of a second to predict all the QCs. For ADA and RF the

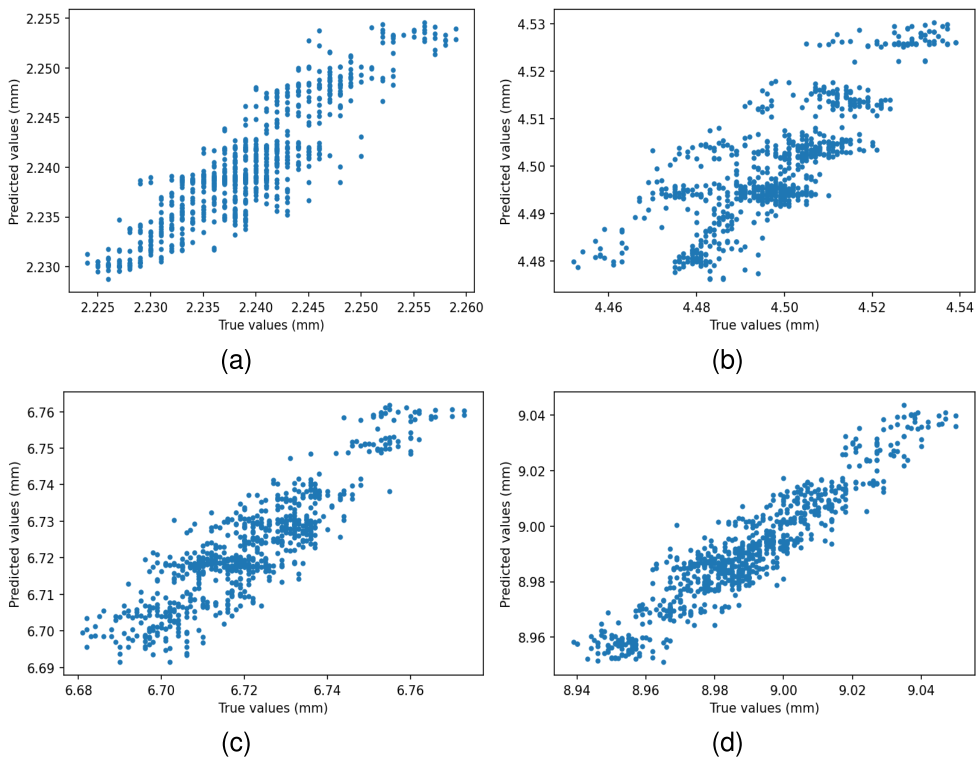

Fig. 8. Comparison between true and predicted lengths for each piece in the test set, using the best model and the best combination of press curve and environmental features. (a) Length 1. (b) Length 2. (c) Length 3. (d) Length 4.

worst average prediction time is 0.0169 (Lengths 2 and 3) and 0.0306 s (Length 3), respectively. Hence, in this case, as for the mass, the considered models can be used in a real-time scenario. In fact, taking into consideration the time taken to produce a workpiece, which for the highest stroke rate (i.e., 35) is ≈1.7 s, this time is much longer than the time required by the proposed models to estimate the QCs.

TABLE X

TRAINING AND PREDICTION TIMES IN SECONDS FOR THE EXECUTION OF THE THREE MODELS WHEN THEY ARE CONFIGURED WITH THE BEST HYPERPARAMETERS SETTINGS: LENGTHS QCS PREDICTION AND BY USING BOTH THE PRESS CURVE AND THE ENVIRONMENTAL FEATURES

Length 1			
Model	**Training**	**Prediction (avg)**	**Prediction (std)**
RF	5.0554	0.0092	0.0006
Ada	1.3419	0.0169	0.0001
GB	14.7979	0.0003	0
Length 2			
Model	**Training**	**Prediction (avg)**	**Prediction (std)**
RF	7.6851	0.0137	0.0009
Ada	1.4896	0.0114	0.0002
GB	8.8951	0.0003	0
Length 3			
Model	**Training**	**Prediction (avg)**	**Prediction (std)**
RF	7.6197	0.0137	0.0009
Ada	2.8108	0.0306	0.0007
GB	14.5123	0.0004	0
Length 4			
Model	**Training**	**Prediction (avg)**	**Prediction (std)**
RF	3.4839	0.0046	0.0002
Ada	2.1036	0.0223	0.0004
GB	40.3309	0.0005	0

VI. DISCUSSION

We now summarize the main results of the analysis performed in this article. We start by highlighting the main findings and discussing some of the identified issues. We first summarize the results of the correlation analysis (see Table V). The press curve features mostly correlated with the mass QCs are related to the removal of the workpiece. This happens because the ejection of the produced workpiece and the filling phase for the subsequent workpiece production are occurring in parallel. Therefore, every produced workpiece correlates with its preceding one. Besides, the correlations between press curve features and the lengths are high for force and work during the ejection and workpiece removal phases. This is expected since higher compaction forces lead to higher elastic relaxations, which is also known as the spring-back factor. The spring-back factor leads to an axial and radial elastic relaxation meaning that the workpiece expands already within the cavity leading to higher ejection force.

Conversely, by analyzing the correlation of the environment features and the QCs we have found that the environment variables are not correlated with the mass and Length 1. However, there is a low and moderate correlation between these variables and Lengths 2–4. This is due to the nature of the powder: it is a mixture of iron particles, press additives, and lubricant. Lubricant is susceptible to environmental conditions, e.g., with humidity the iron density in the powder mixture is

TABLE XI
SUMMARY OF THE GB MODEL PERFORMANCE: RMSE (%)

	Quality characteristics				
Features	Mass	Length 1	Length 2	Length 3	Length 4
Press curve + Env.	0.1455	0.1449	0.2134	0.1185	0.0886

TABLE XII
PREDICTION TIME (AVERAGE) IN SECONDS FOR GB

	Quality characteristics				
Features	Mass	Length 1	Length 2	Length 3	Length 4
Press curve + Env.	0.0003	0.0003	0.0003	0.0003	0.0004

low (lubricant particles are larger). This affects the workpiece length after compaction.

Regarding the ML models, we observe that RF and GB have similar performance when predicting the various QCs, even if they use different combinations of features. Hence, for the sake of clarity, we here summarize our ML-based analysis findings by referring to the GB model only.

Table XI shows the performance of the GB model in terms of RMSE (%), for all the QCs. We have obtained acceptable RMSE (%) for all the considered characteristics, with the lowest RMSE (%) of 0.0886 for the Length 4 characteristic. The measured prediction errors are acceptable because they still ensure properly detect if the QCs of a produced workpiece fall between the upper and lower tolerance limits described in Table I.

Table XII shows the prediction times for the GB model to forecast the five considered QCs. These short times make the proposed approach usable at run time. We note that the reported execution times do not take into account the processing time required to collect the data from the sensors (e.g., raw press curves data), which is, however, very small. Our proposed QCs estimation method is extremely quick since the time needed to compute the target estimations for a workpiece is small compared to the cycle time, which is ≈1.7 s, for the highest stroke rate, i.e., 35 pieces/min.

VII. CONCLUSION AND FUTURE WORK

In the powder compaction process, it is extremely important to carry out regular quality checks and manual adjustments of levels' trajectories. This activity is necessary to meet the challenges posed by the continuous variations of the operating conditions (varying temperature, stroke rate, powder quality, etc.) and ensure adequate consistency in the quality of the produced workpieces over a longer period.

In this article, we have proposed an accurate and lightweight ML-based pipeline to assess the quality (mass and lengths) of sintered workpieces in the compaction process. Our pipeline exploits ML models, and three of them have been compared: RF, ADA, and GB. The models have been trained on a combination of workpiece features, describing the press curve operation and the environment state (humidity, pressure, and temperature), to estimate the mass and lengths of the produced workpieces. On our dataset, we have estimated the RMSE (%), of the compared models, and by using the best ML model, namely GB, this error ranges from a minimum of 0.0886 to a maximum of 0.2134 (see Table XI). Our quality estimation scheme is lightweight as it takes few microseconds (≈300) to estimate the QCs of a produced workpiece. We first note that the measured prediction errors ensure that the estimated QCs can be assessed with enough precision to keep them between the upper and lower tolerance limits. Second, we observe that the estimation is made quickly enough so that it takes less time to compute it than the time required to produce a workpiece at the fastest stroke rate of 35 strokes/min, namely ≈1.7 s.

The analysis presented in this article was performed offline, as it was not possible to interfere with industrial production. Now that we have shown promising results from our offline analysis, we plan to develop an automatic digital control system capable to ensure the desired quality of the produced workpieces, in real-time. Furthermore, we plan to conduct more rigorous experiments to: 1) perform a long-term assessment of the proposed approach; 2) check the generalization capability of the selected model (reuse the model with other types of workpieces); and 3) use even more advanced ML algorithms, such as incremental induction trees, to be able to continuously update the predictive model without retraining it on the full historical dataset. We leave this experimentation in the real-time settings, along with dealing with the computational constraints related to memory usage and power consumption, for future work.

REFERENCES

[1] K. Erhard, *Metals Handbook: Powder Metallurgy*, vol. 7. Detroit, MI USA: ASM International, 1999.

[2] A. Hamweendo, T. Malama, and I. Botef, "Titanium-nickel alloys for bone tissue engineering application via cold spray," in *Proc. Int. Conf. Competitive Manuf.*, 2016, pp. 273–279.

[3] A. Géron, *Hands-on Machine Learning With Scikit-Learn, Keras, and TensorFlow*. O'Reilly, 2009.

[4] P. Beiss, *Pulvermetallurgische Fertigungstechnik*. Berlin, Germany: Springer, 2013.

[5] S. Manlangit, S. Azam, B. Shanmugam, K. Kannoorpatti, M. Jonkman, and A. Balasubramaniam, "An efficient method for detecting fraudulent transactions using classification algorithms on an anonymized credit card data set," in *Proc. Int. Conf. Intell. Syst. Design Appl.* Cham, Switzerland: Springer, 2017, pp. 418–429.

[6] K. G. Sheela and A. R. Varghese, "Machine learning based health monitoring system," *Mater. Today, Proc.*, vol. 24, pp. 1788–1794, Jan. 2020.

[7] R. Kieffer and W. Hotop, *Pulvermetallurgie Und Sinterwerkstoffe*, vol. 9. Berlin, Germany: Springer, 2013.

[8] A. B. Höganäs, "Production of sintered components," Hoegenaes, Höganäs, Sweden, Tech. Rep., 2013.

[9] W. Schatt, K. P. Wieters, and B. Kieback, *Pulvermetallurgie*. Berlin, Germany: Srpinger, 1994.

[10] B. Al-Mangour, "Powder metallurgy of stainless steel: State-of-the art, challenges, and development," in *Stainless Steel: Microstructure, Mechanical Properties and Methods of Application*. New York, NY, USA: Nova, 2015, pp. 37–80.

[11] R. J. Brook, "Sintering: An overview," in *Concise Encyclopedia of Advanced Ceramic Materials*. Amsterdam, The Netherlands: Elsevier, 1991, pp. 438–440.

[12] R. de Oro Calderon, C. Gierl-Mayer, and H. Danninger, *Fundamentals of Sintering: Liquid Phase Sintering*, A. Caballero, Ed. Oxford, U.K.: Elsevier, 2022, pp. 481–492.

[13] B. James, "What is sinter hardening?" *Metal Powder Rep.*, vol. 1, no. 54, p. 38, 1999.

[14] PM Modnet Modelling Group, "Comparison of computer models representing powder compaction process: State of the art review," *Powder Metall.*, vol. 42, no. 4, pp. 301–311, 1999.

[15] S. Sivasankaran, K. Sivaprasad, R. Narayanasamy, and V. K. Iyer, "Evaluation of compaction equations and prediction using adaptive neuro-fuzzy inference system on compressibility behavior of AA 6061_{100-x}-X wt.% TiO_2 nanocomposites prepared by mechanical alloying," *Powder Technol.*, vol. 209, nos. 1–3, pp. 124–137, May 2011.
[16] W. Wang, P. Liu, H. Qi, J. Liu, T. Liu, and L. Zheng, "Finite element analysis of densification of Fe-40at%Al composite powders," *AIP Adv.*, vol. 9, no. 1, Jan. 2019, Art. no. 015311.
[17] M. T. Yan, Y. S. Liao, and C. C. Chang, "On-line estimation of workpiece height by using neural networks and hierarchical adaptive control of WEDM," *Int. J. Adv. Manuf. Technol.*, vol. 18, no. 12, pp. 884–891, Dec. 2001.
[18] S. V. Buuren and K. Groothuis-Oudshoorn, "mice: Multivariate imputation by chained equations in R," *J. Stat. Softw.*, vol. 45, no. 3, pp. 1–67, 2011.
[19] F. Pedregosa et al., "Scikit-learn: Machine learning in Python," *J. Mach. Learn. Res.*, vol. 12, pp. 2825–2830, Nov. 2011.
[20] R. Rousseau, L. Egghe, and R. Guns, "Chapter 4—Statistics," in *Becoming Metric-Wise*. East Yorkshire, U.K.: Chandos, 2018, pp. 67–97.
[21] D. Massimo and F. Ricci, "Popularity, novelty and relevance in point of interest recommendation: An experimental analysis," *Inf. Technol. Tourism*, vol. 23, no. 4, pp. 473–508, Dec. 2021.
[22] Z.-H. Deng et al., "Machine-learning-assisted prediction of the mechanical properties of Cu–Al alloy," *Int. J. Minerals, Metall. Mater.*, vol. 27, no. 3, pp. 362–373, Mar. 2020.
[23] T. Kamal and A. Upadhyaya, "Machine learning based sintered density prediction of bronze processed by powder metallurgy route," *Met. Mater. Int.*, vol. 29, no. 6, pp. 1761–1774, Jun. 2023.
[24] D. S. Leininger, F. Reissner, and J. Baumgartner, "New approaches for a reliable fatigue life prediction of powder metallurgy components using machine learning," *Fatigue Fract. Eng. Mater. Struct.*, vol. 46, no. 3, pp. 1190–1210, Mar. 2023.
[25] W. Wang, H. Qi, P. Liu, Y. Zhao, and H. Chang, "Numerical simulation of densification of Cu–Al mixed metal powder during axial compaction," *Metals*, vol. 8, no. 7, p. 537, Jul. 2018.
[26] I. N. Popescu and R. Vidu, "Compaction behaviour modelling of metal-ceramic powder mixtures. A review," *Sci. Bull. Valahia Univ.-Mater. Mech.*, vol. 16, no. 14, pp. 28–37, Apr. 2018.
[27] J. Almanstötter, "A modified Drucker–Prager cap model for finite element simulation of doped tungsten powder compaction," *Int. J. Refractory Met. Hard Mater.*, vol. 50, pp. 290–297, May 2015.
[28] L. Breiman, "Random forests," *Mach. Learn.*, vol. 45, pp. 5–32, Oct. 2001.
[29] R. E. Schapire, "Explaining AdaBoost," *Empirical Inference*, N. V. Vladimir, Ed. Berlin, Germany: Springer, 2013, pp. 37–52.
[30] A. V. Konstantinov and L. V. Utkin, "Interpretable machine learning with an ensemble of gradient boosting machines," *Knowl.-Based Syst.*, vol. 222, Jun. 2021, Art. no. 106993.
[31] (2021). *10 Machine Learning Algorithms to Know in 2023*. [Online]. Available: https://www.coursera.org/articles/machine-learning-algorithms

David Massimo is currently an Assistant Professor of computer science with the Faculty of Engineering, Free University of Bozen-Bolzano, Bolzano, Italy. His research interests lie in designing, developing, and evaluating recommender and decision-support systems, with particular attention to tourism applications. The outcomes of his research are published in recognized journals and conference proceedings. The recommendation technology he developed has been industrialized.

Prof. Massimo was awarded two best papers by the IFITT Federation for his research contribution to eTourism.

Elias Ganthaler was born in Brunico, Italy. He received the B.Sc. degree from the University of Innsbruck, Innsbruck, Austria, in 2016, and the M.Sc. degree in engineering in mechatronics from University for Health Sciences and Health Technology, Austria, in 2019. He is currently pursuing the Ph.D. degree from the Department of Human-Centered Technologies and Machine Intelligence, Free University of Bozen-Bolzano, Bolzano, Italy.

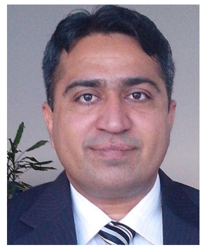

Attaullah Buriro received the B.Eng. degree in telecommunications and electronics from the Mehran University of Engineering and Technology, Jamshoro, Pakistan, in 2001, the M.Eng. degree from the NED University of Engineering and Technology, Karachi, Pakistan, in 2011, and the Ph.D. degree in information and communication technology (security and privacy) from the University of Trento, Trento, Italy, in February 2017.

He is currently an Assistant Professor with the Free University of Bozen-Bolzano, Bolzano, Italy. He has developed several secure, user-friendly, and implicit behavioral biometric-based authentication solutions for smartwatches, smartphones, and critical infrastructures. His research interests includes biometrics, machine learning in cyber security, the Internet of Things (IoT), and recommender systems.

Francesco Barile received the Ph.D. degree in computer science from the University of Naples Federico II, Naples, Italy, in 2018. His Ph.D. thesis entitled A Framework for Group Context-Aware Recommender Systems.

He is currently an Assistant Professor with Maastricht University, Maastricht, The Netherlands. Before, he was a Researcher with the Free University of Bozen-Bolzano, Bolzano, Italy. His research interests focus on explainable artificial intelligence, in particular regarding explainable group recommender systems, explainable multistakeholder recommender systems, decision support systems, user and group modeling, and intelligent user interfaces.

Marco Moraschini received the B.Sc. degree in computer engineering and M.Sc. degree in biomedical engineering from the University of Pavia, Pavia, Italy, in 2010 and 2013, respectively.

He is currently a Data Scientist working as a consultant. Before, he was a Research Assistant with the Faculty of Computer Science, University of Bozen-Bolzano, Bolzano, Italy. He started his career as a Software Developer before transitioning to data science; since then he has worked on various topics, including bioinformatics, computer vision and medical image processing, predictive maintenance, decision support in biomedicine, and NLP.

Anton Dignös (Member, IEEE) received the B.Sc. degree in applied computer science and the M.Sc. degree in computer science from the Free University of Bozen-Bolzano, Bolzano, Italy, in 2008 and 2010, respectively, and the Ph.D. degree in computer science from the Department of Computer Science, University of Zurich, Zürich, Switzerland, in 2014.

He is currently an Assistant Professor with the Database Systems Research Group, Faculty of Engineering, Free University of Bozen-Bolzano. His research interests include interval-timestamped temporal databases, time series data, and data analytics.

Thomas Villgrattner (Member, IEEE) was born in Bozen, Italy. He received the Diploma Engineering degree in electrical engineering and information technology and the Doctor of Engineering degree in mechanical engineering from the Technical University of Munich, Munich, Germany, in 2005 and 2010, respectively, and the master's degree in management from the FernUniversität Hagen, Hagen, Germany, in 2019.

He worked as a Post-Doctoral Researcher with the Technical University of Munich until 2012. From 2012 to 2018, he was working with KUKA Laboratories/Robotics as Product Owner Mechatronics and Research and Development Project Leader. In 2018, he joined GKN Powder Metallurgy, Bolzano, Italy, where he is currently filling the role of the Head of adaptive technology.

Angelika Peer (Member, IEEE) received the Diploma Engineering degree in electrical engineering and information technology and the Doctor of Engineering degree from the Technical University of Munich, Munich, Germany, in 2004 and 2008, respectively.

She has been a Full Professor with the Faculty of Engineering, Free University of Bozen-Bolzano, Bolzano, Italy, since November 2017. From 2014 to 2017, she was a Full Professor with the Bristol Robotics Laboratory, University of the West of England, Bristol, U.K., and before a Senior Researcher and a Lecturer with the Institute of Automatic Control Engineering and a TUM-IAS Junior Fellow of the Institute of Advanced Studies, Technical University of Munich. Her research interests include robotics, control, and human–system interaction.

Francesco Ricci is currently a Full Professor with the Faculty of Engineering, Free University of Bozen-Bolzano, Bolzano, Italy. He has established a reference point for the research on recommender systems in Bolzano. He was a Senior Researcher and the Technical Director of the E-commerce and Tourism Research Laboratory (eCTRL), ITC-IRST, Trento, Italy, from 2000 to 2006. He is the author of more than 200 refereed publications. According to Google Scholar, he has an H-index of 60 and around 25 000 citations. His research interests include recommender systems, user modeling, machine learning, and ICT applications to travel and tourism.

Prof. Ricci has been active with this community as the President of the Steering Committee of the ACM Conference on Recommender Systems from 2007 to 2010. He is the Coeditor of the *Recommender Systems Handbook* (Springer 2011, 2015, and 2022).

Open Access funding provided by 'Libera Università di Bolzano' within the CRUI CARE Agreement